# Atomic core-polarization effects in metastable hadronic helium atoms

Toshimitsu Yamazaki
*Institute for Nuclear Study, University of Tokyo, Tanashi, Tokyo 188, Japan*

Kazumasa Ohtsuki
*Department of Chemistry, Hokkaido University, Kita-ku, Sapporo 060, Japan*
(Received 2 December 1991)

A theoretical consideration is presented concerning the atomic core-polarization effect on the $E1$ transitions of large-$l$ circular orbitals in hadronic helium atoms ($e^-X^-He^{2+}$), where the $e^-$ occupies the $1s$ orbital and the negative hadron ($X^-$) occupies a large-$l$ circular orbital. The first-order mixing of the $2p$ electron configuration due to the repulsive $e^-$-$X^-$ interaction gives rise to a substantial suppression ($\sim\frac{1}{3}$) of the $E1$ transitions, compared with a single-particle estimate, since the slowly moving particle ($X^-$) polarizes the electron cloud in the opposite direction. Recently discovered metastable states of antiprotonic helium atoms are discussed.

PACS number(s): 36.10.−k, 31.30.−i

## I. INTRODUCTION

The trapping of negative kaons ($K^-$) by metastable states formed in liquid helium has recently been discovered [1]; similar phenomena have subsequently been observed in the cases of negative pions ($\pi^-$) [2] and antiprotons ($\bar{p}$) [3]. In particular, the case of $\bar{p}$ is spectacular, since the time distribution of delayed annihilation has revealed that antiprotons in liquid helium survive for up to 15 $\mu$sec, indicating the presence of a series of metastable states. The mean lifetime of the major, and longest, component was 3$\mu$sec.

The trapping of negative hadrons in liquid helium had been conjectured by Condo [4], who ascribed the hitherto known puzzling phenomena of free decays of $\pi^-$ and $K^-$ in helium bubble chambers to a possible trapping by metastable states of exotic atoms. More specifically, Condo pointed out that in a neutral hadronic helium atom ($e^-X^-He^{2+}$) the negative hadron ($X^-$) occupying large-$l$ states of circular orbitals ($l\sim n-1$) undergo only slow radiative transitions, since the electron ionization energy which is expected to be close to the ionization energy of a helium atom ($I_0=24.6\,\text{eV}=0.90\,\text{a.u.}$) is too large compared with the transition energies to cause fast Auger transitions. The neutrality of this atom, involving one electron, protects it from nuclear absorption due to Stark mixing with the surrounding helium atoms. This model was studied theoretically by Russell [5], who used a variational method to compute the various quantities, but neglected configuration mixing of the electron states. Later, the Born-Oppenheimer approximation was employed by Ahlrichs *et al.* [6] to describe this exotic atom. Recently, a comprehensive calculation was carried out by one of the authors (K.O.) [7], which takes into account the configuration interactions. In this paper we show that the effect of configuration mixing on the transition probabilities is important.

## II. STRUCTURE OF AN EXOTIC HELIUM ATOM AND $E1$ TRANSITIONS

An exotic helium atom [$e^-X^-He^{2+}$ ($=X^-He^+$)] is formed when one of the electrons of a target helium atom is replaced by a negative hadron ($X^-$). The $X^-$ occupies one of the large-$n$ atomic orbits located in the same space as the $1s$ electron. The most probable orbit under this condition has a principal quantum number ($n$) close to

$$n_0=(M^*/m_e)^{1/2}\,, \tag{1}$$

where $M^*$ is the reduced mass of $X^-$. In the following we discuss the case of $\bar{p}$ without any loss of generality. In the case of $\bar{p}^4$He, $M^*/m_e=1468.93$ and $n_0=38$. In the vicinity of $n\sim n_0$ the $e^-$ and the $\bar{p}$ nearly equally share the total binding energy, $4\,\text{Ry}+I_0=79$ eV.

For a given principal quantum number ($n$) the orbital angular momentum ($l$) takes values of $0,1,2,\ldots,n-1$. The last one ($l=n-1$) is called "circular orbital," and is characterized by a nodeless wave function. It deexcites to a lower circular orbital ($n'=n-1$, $l'=l-1$) via an electric dipole ($E1$) transition. The transition energy near the $n=n_0$ circular state is roughly given by

$$\Delta E_n\sim(2/n)39.5\,\text{eV}\,. \tag{2}$$

In the case of $\bar{p}$, it is only 2 eV, much smaller than the ionization energy of a helium atom (24.6 eV).

The transition rate is given by

$$\lambda=\frac{4}{3}\frac{(\Delta E_n)^3}{\hbar^4c^3}|\langle f|E1|i\rangle|^2\,, \tag{3}$$

where $\langle f|E1|i\rangle$ is the transition matrix element from an initial state ($i$) to a final state ($f$).

Hereafter, the antiprotonic state is expressed as $|n,l\rangle_{\bar{p}}$. The $E1$ matrix element in the length form for the transition of $\bar{p}$ from a circular orbital $|l+1,l\rangle_{\bar{p}}$ is given by

 

$$\langle l,l-1|E1|l+1,l\rangle_{\bar{p}}=\frac{1}{2^{1/2}M^*Z}\frac{l^{l+3}(l+1)^{l+2}}{(l+\frac{1}{2})^{2l+3}} . \quad (4)$$

Although the matrix element has a mass scale of $1/M^*$, the dependence on $l$ (approximately $\propto l^2$) gives a factor proportional to $M^*$; the matrix element is thus independent of $M^*$ for $l\sim n_0$.

The next-circular orbitals ($n=l+2,l$) proceed to the two lower states ($n'=n-1$, $l'=l-1$) and ($n'=n-2$, $l'=l-1$), with the following respective transition matrix elements.

$$\langle l+1,l-1|E1|l+2,l\rangle_{\bar{p}}=\frac{1}{2^{1/2}M^*Z}\frac{(l+1)^{l+4}(l+2)^{l+2}}{(l+\frac{3}{2})^{2l+4}}\left[\frac{l}{l+1}\right]^{1/2} \quad (5)$$

and

$$\langle l,l-1|E1|l+2,l\rangle_{\bar{p}}=\frac{1}{2M^*Z}\frac{l^{l+3}(l+2)^{l+2}}{(l+1)^{2l+3}}\left[\frac{1}{l+1}\right]^{1/2} . \quad (6)$$

The latter transitions ($\Delta n=2$) are much slower than the former ones ($\Delta n=1$), despite the larger transition energies for $\Delta n=2$. This feature also persists in less-circular orbitals and characterizes the main stream of the cascade, namely, the $\Delta n=1$ and $\Delta l=1$ transitions dominate in the large-$n$ region. A typical circular state of $\bar{p}$ ($n=38$, $l=37$) has a lifetime of 0.6 $\mu$sec, as calculated by Russell [5].

## III. ATOMIC CORE POLARIZATION

We now consider the effect of the repulsive interaction between $e^-$ and $\bar{p}$ in an intuitive way. First, we notice that $\bar{p}$ undergoes circular motion with a frequency that is $1/n$ times smaller than the typical frequency of the $1s$ electron. This means that the electron follows the motion of $\bar{p}$. In this sense, this atom looks like a peculiar diatomic molecule with nuclear charges of $+2$ and $-1$ and, thus, can be handled by the Born-Oppenheimer approximation. Because of the repulsive interaction, the electron is polarized away from $\bar{p}$; this polarized electron cloud contributes coherently to the $E1$ transition of $\bar{p}$ in a destructive way. This is similar to the well-known core-polarization phenomena in nuclear physics; namely, low-energy transitions are strongly affected by a first-order configuration mixing of the core excitation of the same multipolarity (Arima-Horie mechanism [8]).

In the case of exotic atoms, Leon and Seki [9] studied the effect ("dynamic electron screening") in a general framework. Since the present exotic helium atom provide the simplest situation for "atomic core polarization," we have studied the effect in a more explicit way, both intuitively and quantitatively. First, let us consider it from perturbative viewpoints. The electron is virtually excited from the $1s$ state ($\phi_{1s}^{(e)}$) to the $2p$ state ($\phi_{2p}^{(e)}$), etc., by a repulsive interaction [$V(\mathbf{r}_e,\mathbf{R}_p)$]; the wave functions of the relevant states thus have mixed configurations, as given approximately by

$$\Psi(L+1,L)\cong\phi_{1s}^{(e)}|L+1,L\rangle_{\bar{p}}+c_L\phi_{2p}^{(e)}|L,L-1\rangle_{\bar{p}}+d_L\phi_{2p}^{(e)}|L+2,L+1\rangle_{\bar{p}}+\cdots , \quad (7)$$

where $c_L$ and $d_L$ are the mixing amplitudes which make a first-order contribution to the $E1$ transition. We designate the total orbital angular momentum by $L$; the levels of a given $L$ are assigned "approximate principal quantum numbers," such as $N=L+1$, $L+2$,.... from the lowest (circular) to higher excited states. The mixing amplitudes are expressed by perturbations as

$$c_L=-\frac{\langle\phi_{2p}^{(e)};L,L-1|V(\mathbf{r}_e,\mathbf{R}_p)|\phi_{1s}^{(e)};L+1,L\rangle}{\Delta E_{2p\text{-}1s}^{(e)}-\Delta E_n^{(p)}} \quad (8)$$

and

$$d_L=-\frac{\langle\phi_{2p}^{(e)};L+2,L+1|V(\mathbf{r}_e,\mathbf{R}_p)|\phi_{1s}^{(e)};L+1,L\rangle}{\Delta E_{2p\text{-}1s}^{(e)}+\Delta E_n^{(p)}} , \quad (9)$$

where $\Delta E_{2p\text{-}1s}^{(e)}$ is the $2p$-$1s$ transition energy and $\Delta E_n^{(p)}$ is the transition energy of $\bar{p}$ with a principal quantum number ($n$).

The total $E1$ transition amplitude involves not only that for $\bar{p}$, but also an additional term arising from electron excitation, which contributes coherently as

$$\langle L,L-1|E1|L+1,L\rangle=\langle L,L-1|E1|L+1,L\rangle_{\bar{p}}+(c_L+d_{L-1})\langle 2p|E1|1s\rangle_{(e)} . \quad (10)$$

The sign of the additional contribution is negative, as is expected from the above-mentioned intuitive consideration. Since the mixing amplitude involves the same $E1$ matrix element, ($\langle f|E1|i\rangle_{\bar{p}}$), as that for the $\bar{p}$ transition, the total transition amplitude to the first order in the mixing amplitude is approximately factorized in terms of $\langle f|E1|i\rangle_{\bar{p}}$, and, thus, the transition rate reduces to

$$\lambda=(1-\alpha)\lambda_0 , \quad (11)$$

where $\lambda_0$ is the transition rate without core polarization, and $\alpha$ is a parameter which depends on the $\bar{p}$ transition energy as $1/[(\Delta E_{2p\text{-}1s}^{(e)})^2-(\Delta E_n^{(p)})^2]$.

## IV. CI CALCULATIONS

We have so far discussed the essential characteristics of the atomic core-polarization effect based on both intuitive and perturbational viewpoints. We now show that the results of the configuration-interaction calculation [7] support the above-mentioned viewpoints.

In the following we describe the calculation procedure briefly, while the details will be published elsewhere [7]. The energy eigenvalues $E(N,L)$ were obtained by solving the total Hamiltonian using the configuration-interaction (CI) wave functions expressed in the form

$$\Psi(N,L)=\sum_k C_k\phi_k(\mathbf{r},l_e)\Phi_k(\mathbf{R},l_{\bar{p}}) \quad (|l_e-l_{\bar{p}}|\le L\le l_e+l_{\bar{p}r}) , \quad (12)$$

where $\phi(\mathbf{r},l_e)$ is a primitive Slater-type function (STF) for $e^-$ and $\Phi_k(\mathbf{R},l_{\bar{p}})$ is a $\bar{p}$ orbital which is a linear combination of optimized STFs, obtained by solving the Schrödinger equation,

$$[h(R)+\epsilon_0(R)]\Phi_k(\mathbf{R},l_{\bar{p}})=E_k\Phi_k(\mathbf{R},l_{\bar{p}}) \ . \quad (13)$$

In this equation, $\epsilon_0(R)$ is an adiabatic potential of the $1s_\sigma$ electronic state at a fixed $\bar{p}$ position of $R$ and $E_k$ is the total energy of $|1s_\sigma,n_p l_{\bar{p}}\rangle$ state in the Born-Oppenheimer approximation. In order to calculate $\epsilon_0(R)$, 10 $s$- and 9 $p$-STFs are employed and the $\bar{p}$ orbitals $\Phi_k(R,l_{\bar{p}})$ in Eq. (13) are expanded by 18 STFs. Finally, the CI wave functions (12) consist of 10 $s$-, 9 $p$-, and 8 $d$-STFs as $\phi_k(r,l_e)$ and the first 15 $\bar{p}$ orbitals for each $l_{\bar{p}}$. Of course, all possible angular momenta, $(l_e,l_{\bar{p}})=(s;L)$, $(p;L\pm1)$, and $(d;L,L\pm2)$, are utilized.

The calculated energies $E_k$ in Eq. (13) with an adiabatic potential $\epsilon_0(R)$ are in good agreement with the results of Ahlrichs *et al.* [6]. The differences between the CI results $E(N,L)$ and $E_k$ are so small. This, however, does not mean that the adiabatic treatment is capable of approximating the system well in a wide range of $L$; the contribution of the nonadiabatic coupling excluded in Eq. (13) to the transition rates becomes larger as $L$ decreases.

The circular-orbital states, thus calculated, show substantial polarization. The $\bar{p}$ and $e^-$ wave functions of a typical circular orbital ($N=38$, $L=37$), obtained from Eq. (13), are shown in Fig. 1. The $\bar{p}$ is well localized at $\langle R_p\rangle\sim0.57$ a.u. [Fig. 1(c)], while the $e^-$ is distributed over a wide space. Contour mapping of the electron wave function with respect to the position of $\bar{p}$ is shown in Fig. 1(b); its $z$ component is shown in Fig. 1(a). It can be clearly seen from these figures that the $e^-$ is polarized in a direction opposite to the $\bar{p}$ location. Since this polarization follows the slowly moving $\bar{p}$, the $E1$ amplitude of $\bar{p}$ is greatly compensated for by that of $e^-$.

The calculated lifetimes are presented in Fig. 2, and compared with the lifetimes both with and without a configuration interaction. The typical lifetime of the $N=38$, $L=37$ state is 1.5 $\mu$sec, by a factor of 3 longer than that without configuration interaction. This hindrance factor increases as $L$ decreases, since the $\bar{p}$ transition energy, $\Delta E_n^{(p)}$, increases, while approaching the $2p$-$1s$ excitation energy, $\Delta E_{2p\text{-}1s}^{(e)}$.

The calculated energy levels of the neutral $e^-\bar{p}\,\mathrm{He}^{2+}$ atom ($=\bar{p}\,\mathrm{He}^+$) are shown in Fig. 3. The ground state of $\mathrm{He}^0$ lies at $-2.9$ a.u., and that of $\mathrm{He}^+$ at $-2.0$ a.u., as designated. The degeneracy of the levels for each $n$ is removed; the energy gradually increases with $L$. This indicates that Stark mixing is unlikely in this neutral helium atom.

The circular orbitals proceed to lower states, as shown. The next-circular orbital states ($l=n-2$) proceed mainly to the lower states by just changing $n$ and $l$ by one unit. This tendency persists to the whole domain of the present interest, where the $\bar{p}$ wave function is well localized. Only the transitions without changing the radial node ($\Delta n=\Delta l=1$) are favored.

The level sequence of the ionized $\bar{p}\,\mathrm{He}^{2+}$ atom is also

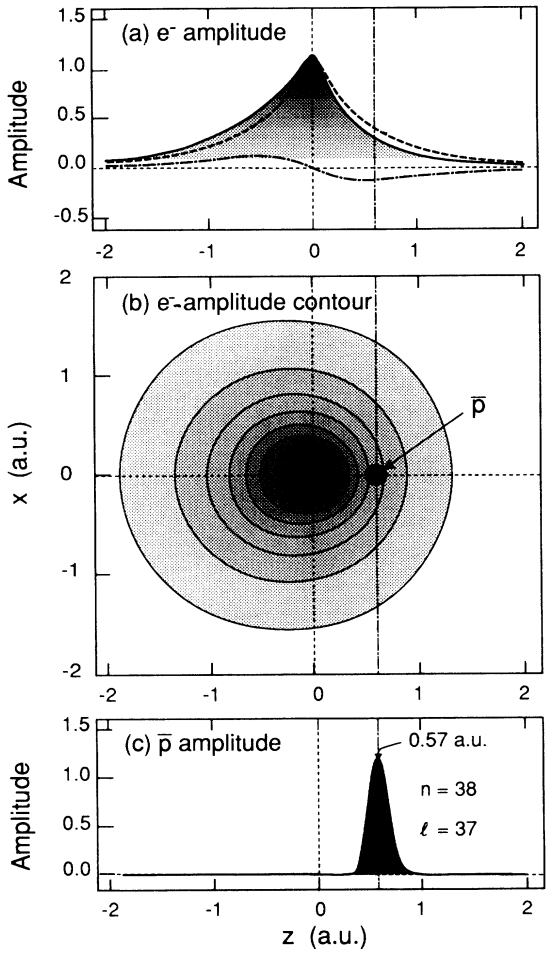


FIG. 1. Spatial distributions of $e^-$ and $\bar{p}$ in a typical circular orbital of the neutral $e^-\bar{p}\,\mathrm{He}^{2+}$ atom ($N=38$, $L=37$), as calculated by solving Eq. (13). (a) Distribution of the wave function of $e^-$ at $x=y=0$ along the $z$-axis (the dashed curve shows unpolarized case). (b) Contour mapping of the $e^-$ wave function in the $x$-$z$ plane in 10 equal steps when $\bar{p}$ is localized on the $z$-axis. (c) Distribution of the wave function of $\bar{p}$; the $\bar{p}$ is seen to be localized at $R_p=0.57$ a.u. on the $z$-axis.

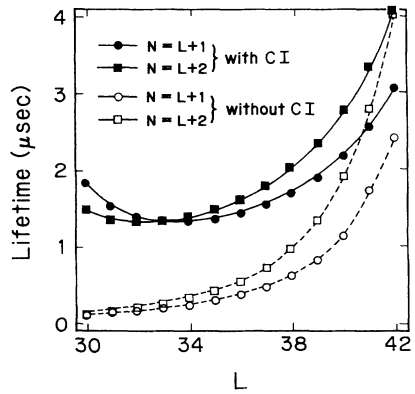


FIG. 2. Calculated lifetimes of the circular states and their vicinities in a neutral $e^-\bar{p}\,\mathrm{He}^{2+}$ atom. Those with and without polarization effects are compared.

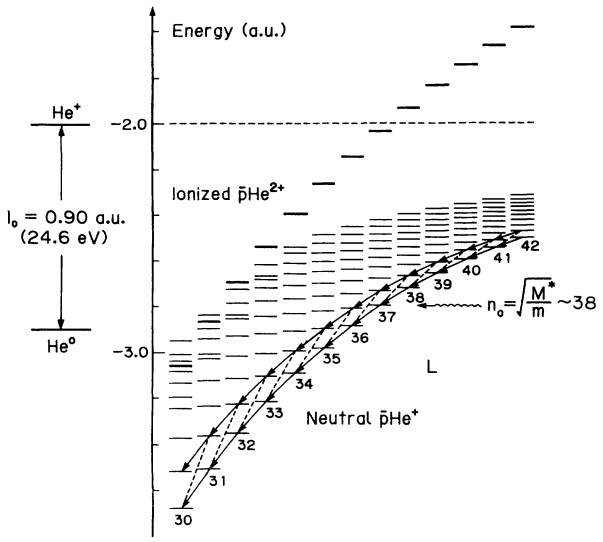


FIG. 3. Calculated energy levels in a neutral $e^-\bar{p}\,He^{2+}$ atom, as designated by the total angular momentum, $L$. The main stream of $E1$ transitions is indicated by arrows. The lowest energy levels of the ionized $\bar{p}\,He^{2+}$ are indicated by bold lines. The ground states of the normal $He^0$ and $He^+$ atoms are at $-2.9$ and $-2.0$ a.u., respectively, as shown.

indicated in Fig. 3 by bold lines. The neutral states with $N\sim 38$, $L\le L_0=31$ ($L_0$ being the angular momentum which divides the metastable and the prompt zones) proceed to ionized states via fast Auger transitions, which are quickly absorbed by the nucleus due to Stark mixing, etc.

## V. TRAPPING FRACTION

The trapping fraction is given by the fraction of populated levels of $L > L_0$, if we know the population, $P(l)$.

The maximum angular momentum ($l_{\max}$) depends on the incident energy ($E$) of $\bar{p}$ during the $\bar{p}$ atom formation, as approximately given by

$$l_{\max}=a_B(2M^*E)^{1/2}/\hbar=10.4[E(\text{eV})]^{1/2} . \tag{14}$$

For $E=17$ eV, for instance, $l_{\max}$ is about 40, marginally exceeding the maximum orbital angular momentum ($L_{\max}=37$) of the $N=38$ levels. Only for $l<l_{\max}$ would we expect that the angular momentum is distributed according to the statistical distribution

$$P(l)=(2l+1),\quad l\le l_{\max} . \tag{15}$$

If this were the case, we would expect that the trapping fraction would be

$$f=1-(L_0/L_{\max})^2\cong 0.3 , \tag{16}$$

which is too large compared with the observed trapping fraction, about 3–4 %.

However, since, in fact, the incident energy during the formation stage is continuously distributed, the distribution of $l$ should deviate from the statistical case. Exotic-atom formation takes place when the energy of $\bar{p}$ reaches somewhere between 0 and $I_0$, where the formation cross section is nearly flat, as shown by Dolinov *et al.* [10]. Since the final stage of a $\bar{p}$ collision just before exotic-atom formation is the ionization loss in the same He medium (minimum loss $\sim I_0$), the energy during the formation stage should be distributed rather uniformly up to 25 eV. Under these circumstances the distribution of $l$ cannot be statistical, but is expected to take a nonstatistical distribution according to

$$P(l)\propto l\ln(l_{\max}/l) . \tag{17}$$

Then, the trapping fraction is given by

$$f=1-\left[\frac{L_0}{L_{\max}}\right]^2\frac{\ln(l_{\max}/L_0)+\frac{1}{2}}{\ln(l_{\max}/L_{\max})+\frac{1}{2}} . \tag{18}$$

If we take $l_{\max}=L_{\max}=37$, we obtain $f=0.04$. This rough estimate is nearly independent of the reduced mass, and accounts fairly well for the observed trapping fractions of about 3% for $\pi^-$, $K^-$, and $\bar{p}$.

## VI. CONCLUDING REMARKS

If there were no collisional quenching, the time distribution of $\bar{p}$ annihilation would be expected to follow a growth-decay type with an overall lifetime that is much longer than the typical single-level lifetime ($\sim 2$ $\mu$sec), since $\bar{p}$ should cascade down through a series of metastable states, as shown in Fig. 3. This is in contrast to the observed shape of the time distribution of delayed $\bar{p}$ annihilation in liquid helium and to the observed lifetime ($\sim 3$ $\mu$sec) of the longest component.

We certainly require further studies: Theoretically, a realistic consideration needs to be made of the formation process and the subsequent collisional excitation-deexcitation processes; and experimentally, the dependence of delayed $\bar{p}$ annihilation on a medium including gaseous phases needs to be examined. To detect the difference between $^4$He and $^3$He would be particularly important. In the present atomic model a difference arises from the reduced mass of $\bar{p}$; the ratio $R=M^*(4)/M^*(3)=16/15$ causes sizable differences in the transition energies and lifetimes. If we assume that the formation mechanism and the subsequent collisional processes are exactly the same for $^3$He and $^4$He, the difference in the lifetime comes from the level lifetime at $n=n_0$ times the level density. A rough estimate (2) yields an overall lifetime of

$$\tau\propto\frac{1}{\lambda}\frac{1}{\Delta E_n}\propto\frac{1}{(\Delta E_n)^4}\propto n_0^4\propto M^{*2} . \tag{19}$$

Thus, we expect that

$$\frac{\tau(^4\mathrm{He})}{\tau(^3\mathrm{He})} \cong R^2 = 1.14 \ . \tag{20}$$

Such a difference can easily be detected, and will provide important information for a better understanding as to whether the observed trapping time is a cumulative atomic cascade time or not.


## ACKNOWLEDGMENTS

We are grateful to Professor R. S. Hayano and members of the experimental group for stimulating daily conversations, and to Professor K. Yazaki for helpful discussions. One of the authors (K.O.) would like to thank Professor K. Ohno and Professor F. Sasaki of the Department of Chemistry of Hokkaido University for their guidance and encouragement.



[1] T. Yamazaki *et al.*, Phys. Rev. Lett. **63**, 1590 (1989).
[2] S. N. Nakamura *et al.*, Phys. Rev. A **45**, 6202 (1992).
[3] M. Iwasaki *et al.*, Phys. Rev. Lett. **67**, 1246 (1991).
[4] G. T. Condo, Phys. Lett. **9**, 65 (1964).
[5] J. E. Russell, Phys. Rev. Lett. **23**, 63 (1969); Phys. Rev. **188**, 187 (1969); Phys. Rev. A **1**, 721 (1970); **1**, 735 (1970); **1**, 742 (1970); J. Math. Phys. **12**, 1906 (1971); Phys. Rev. A **6**, 2488 (1972).
[6] R. Ahlrichs, O. Dumbrajs, H. Pilkuhn, and H. G. Schlaile, Z. Phys. A **306**, 297 (1982).
[7] K. Ohtsuki (unpublished).
[8] A. Arima and H. Horie, Prog. Theor. Phys. **12**, 623 (1954).
[9] M. Leon and R. Seki, Nucl. Phys. A **298**, 333 (1978).
[10] V. K. Dolinov, G. Ya. Korenman, I. V. Moskalenko, and V. P. Popov, Muon Cat. Fusion **4**, 169 (1989).

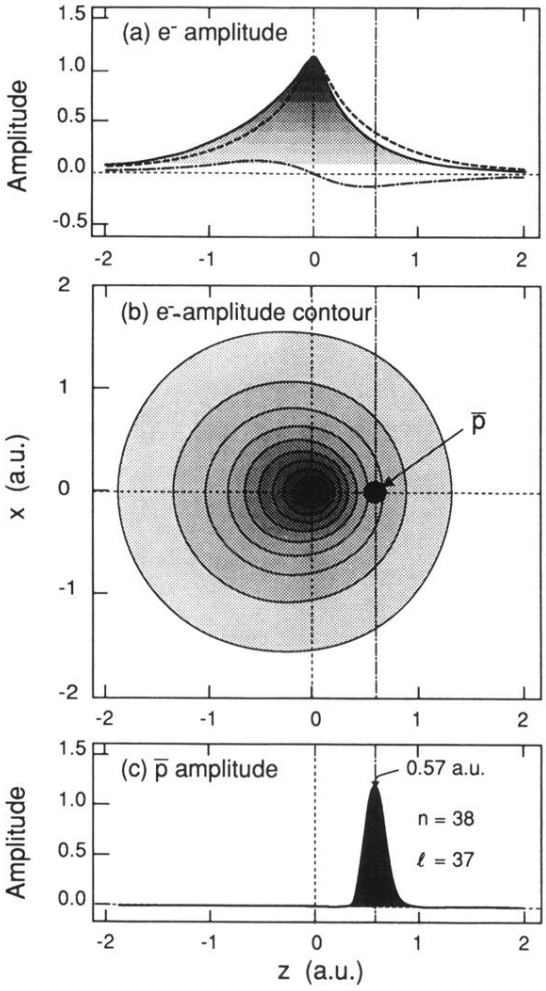


FIG. 1. Spatial distributions of $e^-$ and $\bar{p}$ in a typical circular orbital of the neutral $e^-\bar{p}\,He^{2+}$ atom ($N=38$, $L=37$), as calculated by solving Eq. (13). (a) Distribution of the wave function of $e^-$ at $x=y=0$ along the $z$-axis (the dashed curve shows unpolarized case). (b) Contour mapping of the $e^-$ wave function in the $x$-$z$ plane in 10 equal steps when $\bar{p}$ is localized on the $z$-axis. (c) Distribution of the wave function of $\bar{p}$; the $\bar{p}$ is seen to be localized at $R_p=0.57$ a.u. on the $z$-axis.